ENVIRONMENTAL ENGINEERING SCIENCE
Volume 24, Number 2, 2007

DOI: 10.1089/ees.2006.0033

High-Resolution River Hydraulic and Water Quality Characterization Using Rapidly Deployable Networked Infomechanical Systems (NIMS RD)

Thomas C. Harmon,[1*] Richard F. Ambrose,[2] Robert M. Gilbert,[3] Jason C. Fisher,[1] Michael Stealey,[4] and William J. Kaiser[4]

[1]School of Engineering
University of California, Merced
Merced, CA 95340
[2]Environmental Science & Engineering Program
Department of Environmental Health Sciences
University of California, Los Angeles
Los Angeles, CA 90095-1772
[3]Department of Environmental Health Sciences
University of California, Los Angeles
Los Angeles, CA 90095-1772
[4]Electrical Engineering Department
University of California, Los Angeles
Los Angeles, CA 90095-1594

ABSTRACT

Increasing demands on water supplies, along with concerns about non-point source pollution, and water quality–based ecological factors all point to the need for observing stream flow perturbations and pollutant discharges at higher resolution than has been practical until now. This work presents a rapidly deployable Networked Infomechanical System (NIMS RD) technology for observing spatiotemporal variability in hydraulic and chemical properties across stream channels. NIMS RD is comprised of two supporting towers and a suspension cable delivering power and Internet connectivity for controlling and actuating the tram-like NIMS unit. The NIMS unit is capable of raising and lowering a payload of sensors, allowing a preprogrammed or data-actuated adaptive scan to be completed across a stream channel. In this paper, NIMS RD is demonstrated in two relevant cases: (1) elucidating spatiotemporal variations in nutrients and other biologically significant stream constituents in Medea Creek, a small urban stream in Southern California; and (2) using high-resolution synoptic sampling of steady velocity and salinity distributions across the San Joaquin River in Central California to provide quantitative salt load estimates. For Medea Creek, temperature and specific conductivity (SC) exhibited varying cross-sectional patterns

*Corresponding author: School of Engineering, PO Box 2039, University of California, Merced, CA 95340. *Phone:* 209-724-4337; *Fax:* 209-228-4047; *E-mail:* tharmon@ucmerced.edu

throughout each of three 24 hour scans carried out over three summer months. Both temperature and SC displayed repeating sinusoidal diel fluctuations independent of the spatial variation. For each of the months the cross-sectional variation was less during the late nighttime and morning hours than during the afternoon and early nighttime hours. For the San Joaquin River, high-resolution velocity distributions from NIMS RD were successfully reproduced in separate deployments and quantitatively matched stage-based volumetric flow rates at the site. The product of the velocity and associated SC distributions yielded total salt load estimates similar to previously reported values, but no basis for direct comparison was available.

Key words: stream; river; hydraulics; water quality; confluence; salinity; temperature; robotic sampling

INTRODUCTION

A RAPIDLY DEPLOYABLE NETWORKED infomechanical systems (NIMS RD) technology that facilitates the study of flow and water quality in rivers and streams is introduced in this paper. Degraded river water quality is the norm in the world's populated and agricultural regions due to the impacts of point and non-point source pollution (Laroche *et al*., 1996; Walsh *et al*., 2005). In arid and semi-arid regions, degradation may be exacerbated by decreased dilution caused by upstream water impoundments or withdrawals. Restoring and maintaining river quality in human-dominated regions require striking a balance between river water quality and water supply demands, wastewater disposal needs, groundwater accretions, agricultural drainage flows, and urban runoff. Given the distributed nature of the properties of rivers and their inputs, a major challenge then arises in observing or monitoring water quality changes with sufficient resolution to link those changes to specific events (e.g., reservoir releases) or land management practices (e.g., fertilization). Without a clear link, it is difficult to identify a rational strategy for assigning water quality management objectives.

On a regional or basin scale, using traditional (sparse) gauging station data to calibrate one-dimensional flow and mixing models is a useful approach for estimating downstream flows and water quality based on upstream releases, withdrawals, and returns. For example, this simplistic approach is currently used to manage one of the largest water conveyance systems in the world in Central California (CDWR, 2003). On sub-basin or smaller scales, spatiotemporal variability of velocity and water quality properties results from pollutant inputs, hydrodynamic mixing regimes, and biogeochemical cycling processes that are themselves distributed in time and space. Higher resolution observations are needed if we are to understand processes well enough to predict conditions and manage water quality at these scales (Quinn *et al.,* 2005).

A variety of remote-controlled and autonomous systems exist for transporting water quality sensors through aquatic systems. Buoyed or moored deployment platforms provide vertical profiling capabilities over long time periods at key locations (Honji *et al*., 1987; Luettich, 1993; Doherty *et al*., 1999; Reynolds-Fleming *et al*., 2002). Autonomous underwater vehicles (AUVs) have been used extensively by the oceanographic community, and more recently in lakes and river systems. These robotic devices can be programmed to follow prescribed courses (Laval *et al*., 2000; Yu *et al*., 2002) or to sample adaptively, for example, to track a contaminant plume (Bachmayer *et al*., 2004; Ogren *et al*., 2004; Farrell *et al*., 2005; Sukhatme *et al*., 2006).

There has been less progress in regard to high-resolution autonomous two-dimensional sampling of streams. Data of this nature would be useful in answering many river-related questions, including those pertaining to (1) hydraulics and multi-dimensional river modeling (Hardy *et al.,* 1999, 2003; Hervouet and Bates, 2000), geomorphology, sediment transport, and riparian habitat restoration (Wheaton *et al.*, 2004), and in quantitatively assessing water-quality problems related to point source (e.g., effluent outfalls, agricultural drainage canals) and non-point source (e.g., urban and agricultural runoff). Researchers commonly survey stream velocities by wading or suspending sensors from bridges and boats. In a major effort, De Serres *et al.,* (1999) repeatedly sampled the velocity components in and downstream of a stream confluence zone by erecting a bridge structure that was mounted on dual tracks on the banks. For a river roughly 10–15 m wide by 1 m deep, they made 25–30 three-component velocity measurements on five cross-sections (roughly 150 measurements per survey). Thus, approximately 1800 velocity vectors were measured over the 12 days of this campaign. High-resolution cross-sectional velocity distributions can also be obtained using bottom- and side-mounted acoustic Doppler velocity and similar sonar-based devices. Beyond flow field characterization, however, devices and methods for autonomously mea-

suring coupled hydraulic and water-quality parameters in stream cross-sections efficiently and with high granularity is currently lacking.

The purpose of this paper is to introduce a new technology for obtaining high-resolution observations of spatiotemporal river channel hydraulic and water-quality patterns. NIMS RD is an example of the distributed, embedded networked sensing and actuation technology that has been developed over the past decade to enable pervasive observation of the environment (Szewczyk *et al*., 2004; Culler and Mulder, 2004). This paper describes the NIMS RD device hardware, software, and deployment technique and demonstrates the technology in test cases by mapping the river cross-sectional temperature and salinity at a location on Medea Creek in Southern California and by mapping velocity and salinity on a San Joaquin River channel cross-section in Central California. As the results indicate, the NIMS RD yields reproducible measures of hundreds of spatiotemporally distributed velocity vectors coupled with local water-quality measurements over the course of a few hours.

NIMS RD SYSTEM

Networked infomechanical systems (NIMS) is a broad new research thrust directed at fundamental advances in the ability to monitor and ultimately control environments through distributed sensing and actuation. NIMS introduces a new form of infrastructure-supported mobility that enables sensor nodes to explore and characterize complex, two- and three-dimensional environments. NIMS enables precise, low energy and sustainable motion with an elevated and adjustable perspective. NIMS cableway systems are readily attached to available or installed infrastructure at a cost similar to that of fixed node installation. The availability of infrastructure allows large mass sensor payloads to be manipulated with low energy actuation. Also, NIMS algorithms permit continuous and autonomous control of node position to adapt to characteristically unpredictable environmental events.

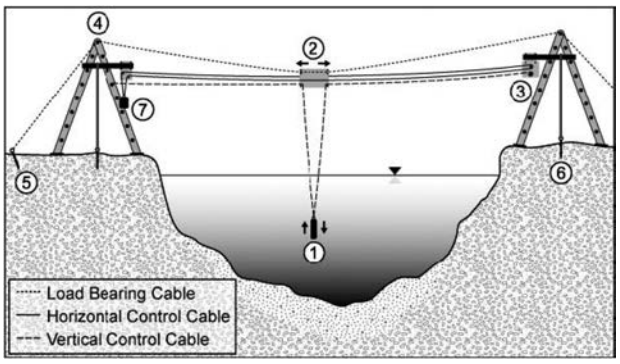

Figure 1. Schematic of the NIMS RD system. The cableway system provides support for the sensor node payload (1). The cableway supports a horizontal actuator (2) controlled by an embedded computing system (3). The cableway is supported by aluminum support towers (4) and anchor systems (5 and 6) while a counterweight (7) provides tension.

The NIMS rapidly deployable (NIMS RD) system (Fig. 1) is an architecture that scales from compact to large scanning range. NIMS RD systems including complex sensor payloads may be deployed with small personnel teams in as little as one to several hours. The NIMS system includes an embedded computing platform providing control to motor systems that actuate the NIMS cable systems for horizontal and vertical transport (Fig. 1). NIMS software systems then proceed, autonomously and in an unattended fashion, to scan sensor nodes through the environment according to either regular sampling patterns or in-field adaptive patterns (Pon *et al*., 2005). Wireless interfaces provide access to user interfaces (via notebook or handheld PDA devices).

DEMONSTRATION SITE SELECTION: RATIONALE AND CHARACTERIZATION

NIMS RD was deployed at a small creek and a moderately large river to test its performance over a wide range of physical conditions. The first deployment was carried out at Medea Creek in Los Angeles County, CA, a small headwater stream in the Malibu Creek Watershed (Fig. 2a). Deploying at Medea Creek provided an opportunity to observe high-resolution stream constituent dynamics in a sub-watershed where the constituent levels are of great public concern due to the level of urbanization occurring in the Malibu Creek Watershed. Medea Creek is listed for algae impairment under Section 303(d) of the Clean Water Act. To control algal biomass, the US Environmental Protection Agency is in the process of decreasing the total maximum daily loads for nutrients in Malibu Creek. In addition to the research and regulatory interests, the site also provided an opportunity to tackle challenges of deploying in densely vegetated and steeply sloped riparian environments.

The second deployment was executed over a 55 m span across the San Joaquin River, immediately below its confluence with the Merced River (Fig. 2b). This site was selected because it provided a challenge for the NIMS RD at a larger scale, and because it afforded an opportunity to develop detailed observations of the hydrodynamic mixing in a river cross-section downstream of the confluence of rivers of distinctly differing water quality. Flow in the San Joaquin River is dominated by agricul-

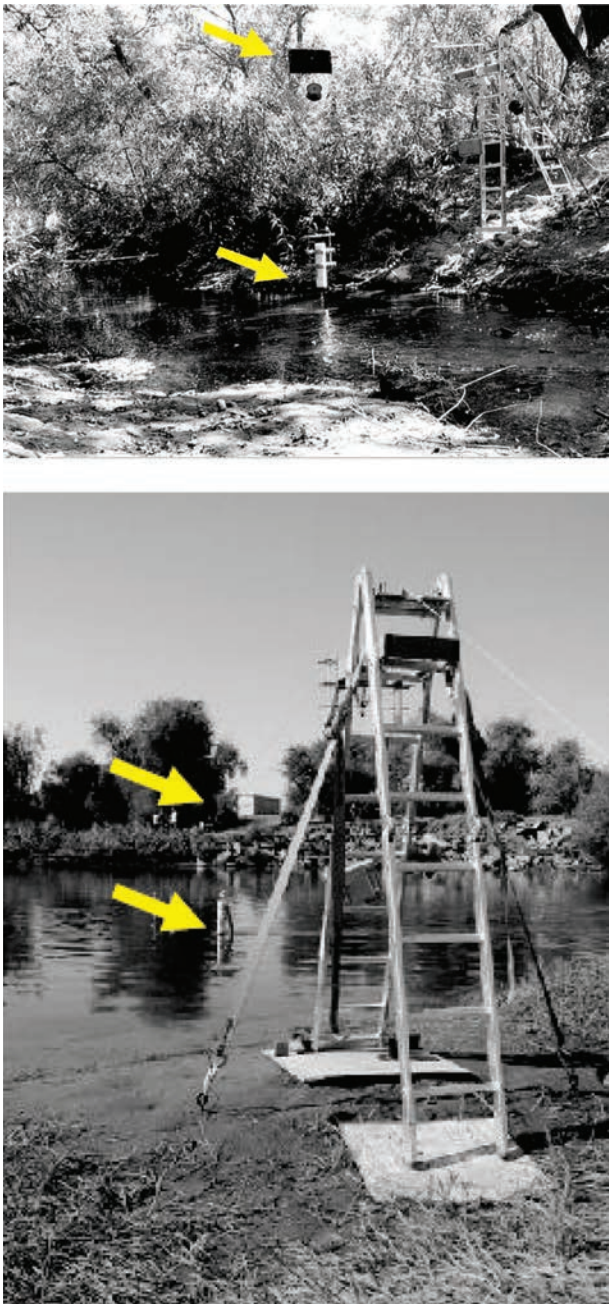

Figure 2. Photographs of the NIMS RD Medea Creek 5 m span deployment (top) and San Joaquin River 55 m span deployment (bottom). Arrows denote location of the NIMS RD cableway and underlying sensor payload.

tural and managed wetland drainage in the late fall. Its flow tends to diminish while the river water increases in temperature and salinity at this time of the year. The Merced River, in contrast, is relatively cold and less saline as it enters the San Joaquin. The two rivers had comparable flows at the time of the deployment (October 6–7, 2005), resulting in a visually distinct mixing zone roughly midway across the confluence zone.

In both deployments, the NIMS RD carried a multiparameter water-quality probe (Hach Environmental, MiniSonde 4a, Loveland, CO) equipped with temperature, conductivity (specific conductance, or SC), nitrate, ammonium, and pH sensors. For the San Joaquin River deployment, an acoustic Doppler velocity sensor (Sontek Triton ADV, San Diego, CA) was also suspended from the NIMS RD unit at the same level and just upstream of the water-quality probe. This work focuses on the temperature and SC for the Medea Creek deployment and on velocity and SC for the San Joaquin River. The temperature sensor in the MiniSonde was a stainless-steel variable resistance thermistor (accuracy $\pm$ 0.1°C; resolution 0.01°C). The SC sensor was an open-cell graphite electrode design with a working range of 0 to 100 μS/cm (accuracy $\pm$ 0.5% measured value; resolution 0.001 μS/cm). The velocity sensor has a working range of 0.001 to 6 m/s (accuracy $\pm$ the greater of 0.1% measured value or 1 mm/s; resolution 0.1 mm/s).

The NIMS RD delivers sensors to depths below the water surface using a predetermined sampling grid or adaptive sampling algorithms. Regular sampling grids were employed in both deployments. For Medea Creek, the sample grid was determined *in situ* at the beginning of each deployment. A plumb line was used to determine the sample points. The plumb line was shuttled across the stream at 20 cm intervals from bank to bank. At each interval the distance from the water line to the creek bottom was determined. Sample points were assigned every 20 cm for each of the vertical transects. The resulting 20 cm by 20 cm grid (64 points) required 25 min for each scan. For the San Joaquin River deployment, a kayak-based echo-sounder operating at 210 kHz (Valeport, Midas Surveyor, Devon, UK) was used to map the river bottom and design relatively sparse and fine sampling grids in order to test the effects of sampling density. The sparse sampling was executed on regular 180 cm horizontal by 50 cm vertical spatial intervals (total 53 points) and required ~42 min to complete. Sample spacing for the fine grid was 60 cm by 20 cm (309 total points) and required 3 h, 20 min to scan.

All the sensors utilized on-board data-logging, which could be queried remotely using a wireless palm-scale computer. Similarly, the scripts controlling the NIMS-RD motors wrote time-stamped (x, z) sample coordinates to a log file after every move. Before each deployment, the internal clocks for all sensors deployed were synchronized with the notebook computer that actuated the motor system. Using the time stamp as a common variable between data sets, the (x, z) position log file was combined with the sensors' log files.

To examine cross-sectional patterns, contour plots were constructed from interpolated data points. Interpolation of the Medea Creek data was performed using a gridded bivariate interpolation method, based on an algorithm from Akima (1978) and using a uniform spatial grid for the interpolated data with 0.2 cm resolution. The spatial domain for the Medea Creek contour plots is the convex hull determined by the sampling locations. The gridded bivariate interpolation method was also applied to the San Joaquin River ADV velocity data, but a zero-velocity boundary was assumed at the bathymetric surface. For the SC data, interpolation was implemented with an inverse distance weighted interpolation method (inverse distance weighting power of 3). The spatial grid for the San Joaquin River interpolated data has a 2 cm resolution. In this case, the spatial domain for the contour plots was defined by the bathymetry within the cross-section and the elevation of the water surface. The volumetric flow rate, Q, was calculated using the interpolated velocity distribution as:

$$Q = \sum_{i=1}^{N} \begin{cases} A_i V_i & \text{for i in } \Omega, \\ 0 & \text{otherwise.} \end{cases} \quad (1)$$

where N is the total number of grid elements, A_i is the area of element i, V_i is the water velocity of element i, and Ω is the spatial domain of the cross-section. Similarly, the TDS flux or load (F) is calculated as:

$$F = \sum_{i=1}^{N} \begin{cases} 0.65(SC_i)A_iV_i & \text{for i in } \Omega, \\ 0 & \text{otherwise.} \end{cases} \quad (2)$$

where SC_i is the specific conductivity of element i, and 0.65 is a conversion factor (μS/cm to mg/L TDS).

RESULTS AND DISCUSSION

For visualizations and analysis, each scan is considered a discrete point in time. This assumption requires relatively short scan durations and constant flow and transport conditions over the course of the scan. For the high-resolution San Joaquin data, flow conditions were constant throughout the deployment according to a downstream gauging station. Salinity conditions entering the confluence were relatively constant according to upstream gauging stations on both rivers. Furthermore, duplicate high-resolution scans on Oct 6 and 7 yielded very similar SC distributions (see discussion below), suggesting that transport conditions were also constant during the course of a high-resolution scan.

Both the Medea Creek and San Joaquin River NIMS RD scans yielded cross-sectional hydraulic and SC distributions at resolutions that would be difficult to obtain manually. The resulting monthly 24 h scans at Medea Creek revealed previously unobserved spatiotemporal stream constituent patterns. For a given constituent, discernable interrelated spatiotemporal patterns on several scales were observed. We focus on electrical conductivity (SC) and temperature (T) to illustrate these patterns and relationships. T and SC showed varying cross-sectional patterns throughout the 24 h scan (examples in Fig. 3). For both parameters, the patterns invert over the 24 h period and seem related to the direction of the temporal patterns described below. To explore temporal patterns, the sample points in each cross-sectional scan were averaged and the average values plotted over time. Both T and SC displayed repeating sinusoidal diel fluctuations independent of the spatial variation (Figs. 4a and 5a). The sinusoidal pattern for T tracks expected air temperature patterns. The sinusoidal pattern for SC is the inverse of the T pattern and exhibits greater variability within the 24 h period. Urban runoff pulses from lawn watering and other outdoor water usage may be a contributing factor to the greater variability of the SC pattern. Seasonal trends of increasing/decreasing amplitude and range of

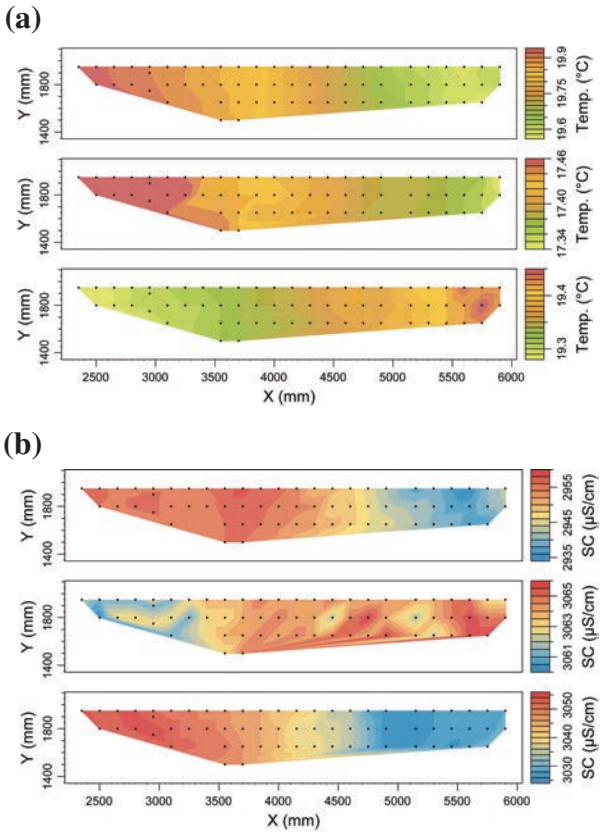

Figure 3. Typical cross-sectional temperature **(a)** and specific conductance **(b)** distributions produced during a 24 h NIMS RD scan of Medea Creek on Sept. 26–27, 2005 at 7:50 a.m. (top), 4:09 a.m. (middle), and 2:55 p.m. (bottom).

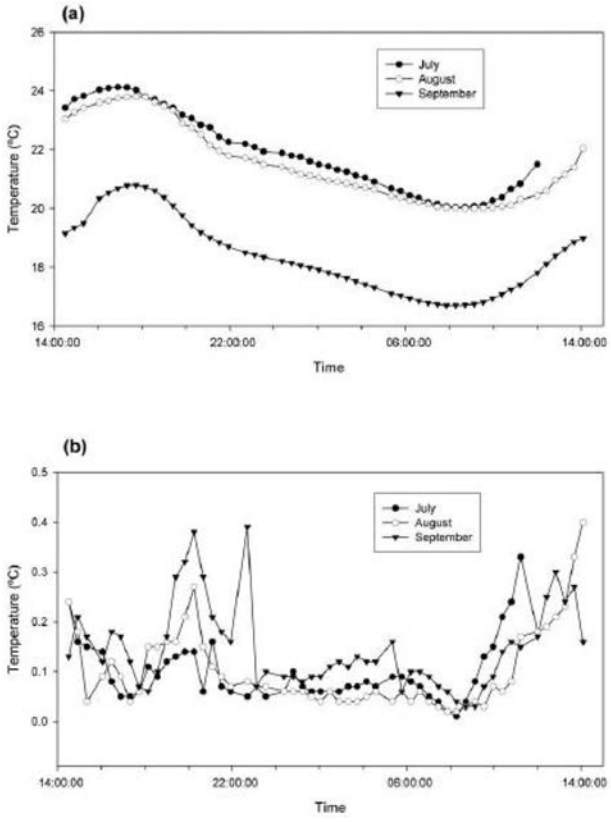

Figure 4. **(a)** Spatially averaged stream temperature variation over 24 h periods in three different months. **(b)** Variation in maximum temperature range ($T_{max} - T_{min}$) observed in cross-sectional NIMS RD scans (both for July, Aug., and Sept. Medea Creek NIMS RD deployments).

the temporal fluctuations were suggested for both T and SC; however, additional monthly deployments are needed to explore the consistency of these seasonal trends.

To investigate how the variation in the cross-section parameter values changed over time, the difference between the maximum and minimum values for each discrete cross-section was calculated and plotted over the 24 h period (Figs. 4b and 5b). The cross-sectional variation was consistently lower during the late nighttime and morning hours than during the afternoon and early nighttime hours. Although both SC and T showed the same general trend, the hours of low variability for T took place a few hours earlier than they did for SC. The mean cross-section range in temperature from 11:00 p.m. to 9:00 a.m. was 0.067°C, which was significantly different from the mean range during the remainder of the 24 h period, 0.158°C (Welch's *t* test for unequal variances on the data pooled for the 3 months, $p < 0.001$). The mean cross-section range in conductivity from 2:30 a.m. to 1:00 p.m. was 9.5 μS, which was significantly different from the mean range during the remainder of the 24 h period, 13.7 μS (Welch's *t* test for unequal variances on the data pooled for the 3 months, $p < 0.001$).

All the aforementioned trends may be a product of any combination of urban influences, biological processes, and chemical processes. Although this observational study does not identify the mechanism(s) behind these trends, it does stimulate hypotheses and demonstrate the importance of considering small-scale spatiotemporal variation for stream monitoring and management. Without considering these spatiotemporal variations, a false conclusion about in-stream conditions could be made, which could lead to suboptimal management practices.

The San Joaquin River low- and high-resolution velocity fields are plotted in Figure 6. As the contouring indicates, the low-resolution field is characterized by some unrealistic patterns, while the higher granularity sampling effort seems to result in more natural patterns. Summary statistics for the two velocity fields are significantly dif-

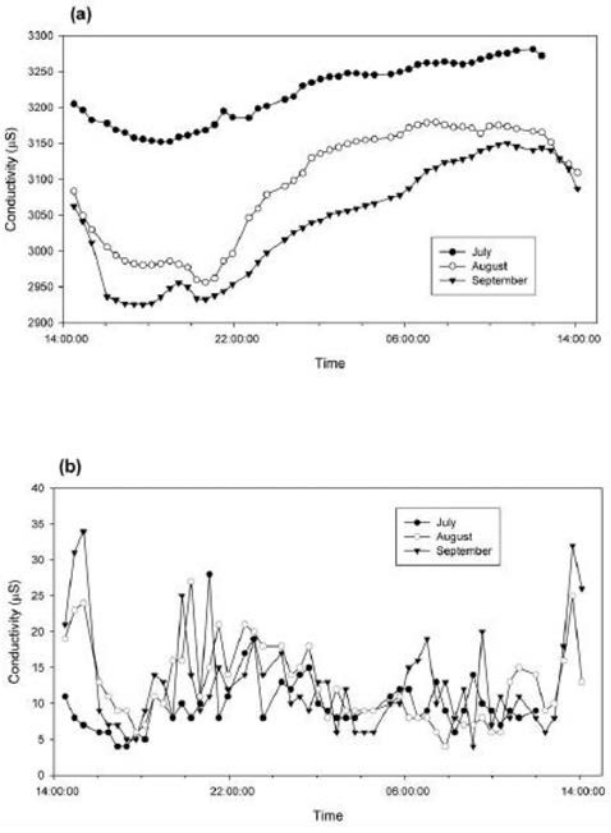

Figure 5. **(a)** Spatially averaged stream specific conductivity (SC) variation over 24-hr periods. **(b)** Variation in maximum SC range ($SC_{max} - SC_{min}$) observed in cross-sectional NIMS RD scans (July, Aug., and Sept. Medea Creek NIMS RD deployments).

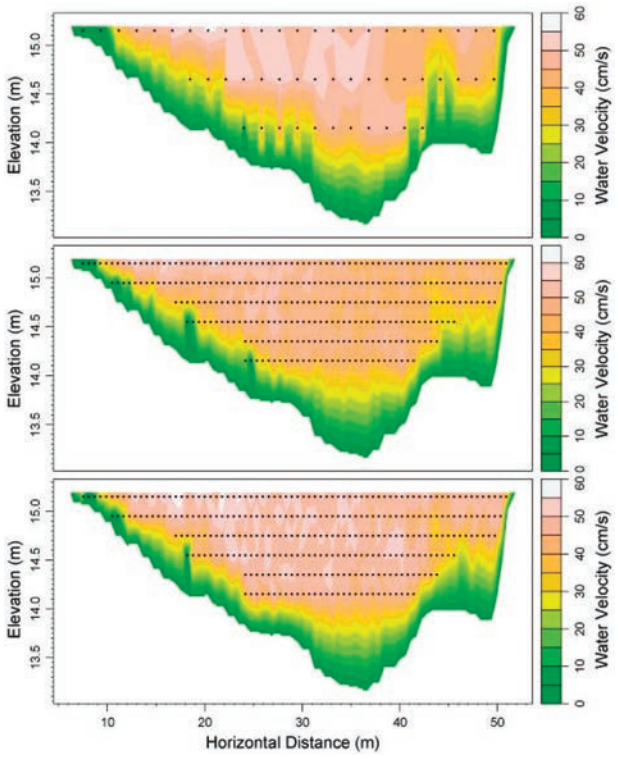

Figure 6. Low-resolution (10/6/05, top) and high-resolution (10/6/05, middle; 10/7/05, bottom) cross-sectional acoustic Doppler velocity (ADV) distributions generated during the San Joaquin River NIMS RD deployment (plot aspect ratio is 10:1).

ferent. The low-resolution velocity scan resulted in maximum and mean velocities of 56.3 and 21.0 (SD 23.8) cm/s, respectively; the corresponding high-resolution results are 60.6 and 36.4 (SD 19.2) cm/s for the Oct 6 scan and 58.3 and 37.8 (SD 19.3) for the Oct 7 scan. The US Bureau of Reclamation Newman gauging station roughly 100 m downstream from the NIMS RD cross-section indicated flow rates of 18.29 and 19.17 m^3/s, respectively (average values based on stage at the time of deployment). The total volumetric flow rate estimated by Eq. (1) for the low-resolution scan was just 4.1% below this value (17.54 m^3/s), and the-high resolution velocity distributions yielded flows nearly the same as the gauging station values (18.38 m^3/s for Oct 6; 19.33 m^3/s, Oct 7).

High-resolution SC scans for the San Joaquin River cross-section for Oct 6 and 7 are plotted in Figure 7. The maximum and mean SC values for the first scan were 1291 and 801 (SD 395) μS/cm, respectively; for the second scan these values were 1244 and 765 (SD 373) μS/cm. Given the lack of significant flow variation over this 2 day period, the consistency of the SC distribution suggests that salinity inputs were constant over the 2 day period, and that the NIMS RD results are reproducible under steady flow conditions. It is worth noting that this point is true in spite of system dismantling and reassembly between the first and second scans (for security).

The total salt loads calculated by combining the information from the velocity and SC scans using Eq. (2) were 9.30 and 9.33 kg/s, respectively. The similarity of these numbers reinforces the reproducibility of the NIMS RD deployment method. Unfortunately, the downstream gauging station that was used to check the volumetric flow rate no longer records SC. However, these values are of the same order of magnitude as those estimated previously for this portion of the San Joaquin River (CDWR, 2003).

CONCLUSIONS

This paper introduces the NIMS RD technology for obtaining high-resolution observations of spatiotemporal river channel hydraulic and water quality patterns. The data collected using the NIMS RD technology would be difficult to obtain in a reproducible manner using manually deployed sensors. The cases investigated here demonstrate that the system is suitable for small streams, yet structurally sound over spans exceeding 50 m. The Medea Creek case also demonstrates several successful autonomous deployments over periods exceeding 24 h. Results for Medea Creek temperature and SC clearly revealed spatiotemporal patterns that would be difficult to observe through continuous, single-point monitoring. The San Joaquin River case demon-

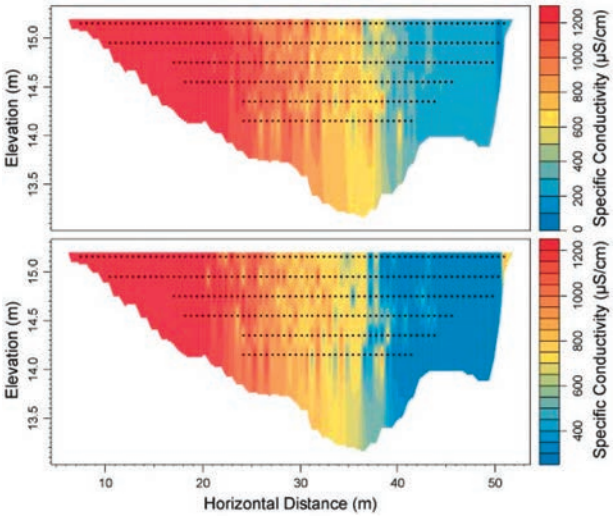

Figure 7. High-resolution (10/6/05, top; 10/7/05, bottom) cross-sectional specific conductivity (SC) distributions generated during the San Joaquin River NIMS RD deployment (plot aspect ratio is 10:1).

strated that the NIMS RD velocity distributions are in quantitative agreement with conventional flow-stage observations. Although analogous data were not available for validating the salt loads associated with SC distributions, the close agreement between the two scans suggests that NIMS RD can be used as a quantitative tool in evaluating distributed water quality properties and chemical fluxes in river systems.

The NIMS RD technology can help to resolve a variety science questions and engineering problems in streams and coastal waterways high-resolution, multi-dimensional spatiotemporal chemical distribution and flux data in support of a variety of stream and coastal waterway investigations. By equipping the NIMS payload with the relevant sensors, such investigations span hydraulic and geomorphologic characterization, pollutant dispersion, and stream reaeration studies, and riparian restoration efforts from the perspective of distributed flow, water, and sediment quality properties. While this paper describes a predetermined sampling strategy, the NIMS RD is also capable of executing adaptive sampling, which may be appropriate when data are time-sensitive. For example, a sewage spill or overflow event might call for a rapid determination of the zone where contamination is above a threshold value or where dissolved oxygen is depleted. In such cases, gradient-based, statistical, or other search algorithms might be employed to rapidly achieve monitoring or observational objectives.

ACKNOWLEDGMENTS

This work was funded by the National Science Foundation through Information Technology Research (ITR): Networked Infomechanical Systems (NIMS) (award no. 0331481), the Center for Embedded Networked Sensing (CENS) (award no. 0120778), and CLEANER: Planning a Multiscale Sensor Network to Observe, Forecast and Manage a CLEANER California Water Cycle (award no. 01414300). Yeung Lam and Eric Yuen (both UCLA) developed the sensor interface and data acquisition systems. Eric Graham (UCLA), Victor Chen (UCLA), and Sandra Villamizar Amaya (UCM) provided assistance in the field. The authors gratefully acknowledge in-kind support from the Merced Irrigation District for cooperation on reservoir operations and the Kelly family for access to the San Joaquin River site.

REFERENCES

AKIMA, H. (1978). A method of bivariate interpolation and smooth surface fitting for irregularly distributed points. *AMC Trans. Math. Software* **4,** 148–164.

BACHMAYER, R., LEONARD, N.E., GRAVER, J., FIORELLI, E., BHATTA, P., and PALEY, D. (2004). Underwater gliders: Recent developments and future applications. *Proceedings of IEEE Int. Symp. Underwater Technol. (UT'04)*. Tapei, Taiwan.

CDWR (2003). *CalSim II Simulation of Historical SWP-CVP Operations*. California Department of Water Resources Technical Memorandum Report, Sacramento, CA, 96 pp.

CULLER, D.E., and MULDER, H. (2004). Smart sensors to network the world. *Sci. Am*. **290,** 84–91.

DE SERRES, B., ROY, A.G., BIRON, P.M., and BEST, J.L. (1999). Three-dimensional structure of flow at a confluence of river channels with discordant beds. *Geomorph* **26,** 313–335.

DOHERTY, K.W., FRYE, D.E., LIBERATORE, S.P., and TOOLE, J.M. (1999). A moored profiling instrument. *J. Atmos. Oceanic Technol*. **16**, 1816–1829.

FARRELL, J.A., PANG, S., and WEI, L. (2005). Chemical plume tracing via an autonomous underwater vehicle. *IEEE J. Oceanic Eng*. **30**, 428–442.

HARDY, R.J., BATES, P.D., and ANDERSON, M.G. (1999). The importance of spatial resolution in hydraulic models for floodplain environments. *J. Hydrol*. **216,** 124–136.

HARDY, R.J., LANE, S.N., FERGUSON, R.I., and PARSONS, D.R. (2003). Assessing the credibility of a series of computational fluid dynamic simulations of open channel flow. *Hydrol. Processes* **17,** 1539–1560.

HERVOUET, J.M., and BATES, P. (2000). The TELEMAC modeling system—Special issue. *Hydrol. Processes* **14,** 2207–2210.

HONJI, H., KANEKO, A., and KAWATATE, K. (1987). Self-governing profiling system. *Cont. Shelf Res*. **7,** 1257–1265.

KAISER, W., POTTIE, G., SRIVASTAVA, M., SUKHATME, G.S., VILLASENOR, J., and ESTRIN, D. (2005). Networked Infomechanical Systems (NIMS) for ambient intelligence. In *Ambient Intelligence.* W. Weber, J.M. Rabaey, and E. Aarts (eds), New York*:* Springer-Verlag.

KNIGHTON, D. (1998). *Fluvial Forms and Processes: A New Perspective*. London/New York: Arnold Publishers, 398 pp.

LAROCHE, A.M., GALLICHAND, J., LAGACE, R., and PESANT, A. (1996). Simulating atrazine transport with HSPF in an agricultural watershed. *J. Environ. Eng. ASCE* **122,** 622–630.

LAVAL, B., BIRD, J.S., and HELLAND, P.D. (2000). An autonomous underwater vehicle for the study of small lakes. *J. Atmos. Oceanic Technol*. **17,** 69–76.

LUETTICH, R.A. (1993). PSWIMS, a profiling instrument system for remote physical and chemical measurements in shallow-water. *Estuaries* **16,** 190–197.

OGREN, P., FIORELLI, E., and LEONARD, N.E. (2004). Cooperative control of mobile sensor networks: Adaptive gra-

dient climbing in a distributed environment. *IEEE Trans. Auto. Contr.* **49,** 1292–1302.

PON, R., BATALIN, M.A., GORDON, J., KANSAL, A., LIU, D., RAHIMI, M., SHIRACHI, L., YU, Y., HANSEN, M., KAISER, W.J., SRIVASTAVA, M., SUKHATME, G., and ESTRIN, D. (2005). Networked infomechanical systems: A mobile embedded networked sensor platform. *Proceedings of the IEEE/ACM Fourth International Conference on Information Processing in Sensor Networks* (IPSN-SPOTS), April 2005, pp. 376–381.

QUINN, N.W.T., JACOBS, K., CHEN, C.W., and STRINGFELLOW W.T. (2005). Elements of a decision support system for real-time management of dissolved oxygen in the San Joaquin River deep water ship channel. *Environ. Model Software* **20,** 1495–1504.

REYNOLDS-FLEMING, J.V., FLEMING J.G., and LUETTICH, R.A. (2002). Portable autonomous vertical profiler for estuarine applications. *Estuaries* **25,** 142–147.

SZEWCZYK, R., OSTERWEIL, E., POLASTRE, J., HAMILTON, M., MAINWARING, A., and ESTRIN, D. (2004). Habitat monitoring with sensor networks. *Commun. ACM* **47,** 34–40.

SUKHATME, G.S., DHARIWAL, A., ZHANG, B., OBERG, C., STAUFFER, B., and CARON, D.A. (2006). The design and development of a wireless robotic networked aquatic microbial observing systems. *Environ. Eng. Sci.* **24**(2), current issue.

WALSH, C.J., ROY, A.H., FEMINELLA, J.W., COTTINGHAM, P.D., GROFFMAN, P.M., and MORGAN, R.P. (2005). The urban stream syndrome: Current knowledge and the search for a cure. *J. N. Am. Benth. Soc*. **24,** 706–723.

WHEATON, J.M., PASTERNACK, G.B., and MERZ, J.E. (2004). Spawning habitat rehabilitation. I. Conceptual approach and methods. *Intl. J. River Basin Manage.* **2,** 3–20.

YU, X.R., DICKEY, T., BELLINGHAM, J., MANOV, D., and STREITLIEN, K. (2002). The application of autonomous underwater vehicles for interdisciplinary measurements in Massachusetts and Cape Cod Bays. *Cont. Shelf Res*. **22,** 2225–2245.